https://doi.org/10.5194/acp-2019-673
Preprint. Discussion started: 7 August 2019

Atmospheric Chemistry and Physics Discussions

Composition and mass size distribution of nitrated and oxygenated aromatic compounds in ambient particulate matter from southern and central Europe – implications for origin

Zoran Kitanovski[1*], Pourya Shahpoury[1,2], Constantini Samara[3], Aristeidis Voliotis[3,4], Gerhard Lammel[1,5]

[1] Max Planck Institute for Chemistry, Multiphase Chemistry Department, Mainz, Germany

[2] Environment and Climate Change Canada, Air Quality Processes Research Section, Toronto, Canada

[3] Aristotle University of Thessaloniki, Department of Chemistry, Environmental Pollution Control Laboratory, Thessaloniki, Greece

[4] University of Manchester, School of Earth and Environmental Sciences, Centre for Atmospheric Sciences, Manchester, United Kingdom

[5] Masaryk University, Research Centre for Toxic Compounds in the Environment, Brno, Czech Republic

[*]now at: Lek Pharmaceuticals d.d., Ljubljana, Slovenia

Correspondence to: Zoran Kitanovski (z.kitanovski@mpic.de); Pourya Shahpoury (p.shahpoury@mpic.de)

Abstract

Nitro-monoaromatic hydrocarbons (NMAHs), such as nitrocatechols, nitrophenols and nitrosalicylic acids, are important constituents of atmospheric particulate matter (PM) water soluble organic carbon (WSOC) and humic-like substances (HULIS). Nitrated and oxygenated derivatives of polycyclic aromatic hydrocarbons (NPAHs, OPAHs) are toxic and ubiquitous in the ambient air; due to their light absorption properties, together with NMAHs they are part of aerosol brown carbon (BrC). We investigated the winter concentrations of these substance classes in size-resolved particulate matter (PM) from two urban sites in central and southern Europe, i.e. Mainz (MZ), Germany and Thessaloniki (TK), Greece. $\sum_{11}$NMAH concentrations in PM_{10} and total PM were 0.51-8.38 and 12.1-72.1 ng m^{-3} at MZ and TK site, respectively, whereas $\sum_{8}$OPAHs were 47-

https://doi.org/10.5194/acp-2019-673
Preprint. Discussion started: 7 August 2019

Atmospheric Chemistry and Physics Discussions

1636 and 858-4306 pg m^{-3}, and $\sum_{17}$NPAHs were ≤90 and 76-578 pg m^{-3}, respectively. NMAHs and the water-soluble OPAHs contributed 0.4 and 1.8%, and 0.0001 and 0.0002 % to the HULIS mass, at MZ and TK, respectively. The mass size distributions of the individual substances generally peaked in the smallest or second smallest size fraction i.e., <0.49 µm or 0.49-0.95 µm. The mass median diameter (MMD) of NMAHs was 0.10 µm and 0.27 µm at MZ and TK, respectively, while the MMDs of NPAHs and OPAHs were both 0.06 µm at MZ, and 0.12 and 0.10 µm at TK. Correlation analysis between NMAHs, NPAHs and OPAHs from one side and WSOC, HULIS, nitrate, sulphate and potassium cation (K^+) from another, suggested that the fresh biomass burning emissions dominated at the TK site, while aged air masses (influenced by biomass and fossil fuel burning) were predominant at the MZ site.

1. Introduction

Atmospheric humic-like substances (HULIS) represent a complex mixture of aliphatic and aromatic compounds with multiple functional groups, such as hydroxyl, carbonyl, carboxyl, nitro, nitrooxy, and sulphate groups (Havers et al., 1998; Graber and Rudich, 2006; Hallquist et al., 2009; Claeys et al., 2012). They are a major constituent of aerosol water-soluble organic carbon (WSOC), contributing between 9 and 72% of WSOC mass (Decesari et al., 2000; Graber and Rudich, 2006; Lin et al., 2010; Zheng et al., 2013). The distribution of HULIS molecular weights (MWs) is unimodal and ranges between 100 and 500 Da with most of the compounds grouping around 200 Da (Graber and Rudich, 2006; Claeys et al., 2012; Song et al., 2018), unlike soil humic and fulvic acids with MW distributions extending well beyond 1000 Da. Due to the presence of light-absorbing polyconjugated and aromatic compounds (Duarte et al., 2005; Graber and Rudich, 2006; Claeys et al., 2012; Zheng et al., 2013), HULIS are an important constituent of aerosol water-soluble brown carbon (BrC; Laskin et al., 2015, and references therein). The intense light-absorption of HULIS in the ultraviolet and violet and blue visible regions, between 200 and 500 nm, can affect aerosol optical properties and atmospheric photochemical processes (Andreae and Gelencser, 2006). Owing to the presence of highly polar polyfunctional material, HULIS has surface-active properties and can make aerosols act as cloud condensation nuclei (CCN). In the aerosol aqueous phase, HULIS can increase the solubility of hydrophobic organic compounds and change the reactivity and solubility of metal aerosols, owing to metal-complexation properties (Graber and Rudich, 2006). Finally, due to the presence of redox-active moieties, HULIS can

https://doi.org/10.5194/acp-2019-673
Preprint. Discussion started: 7 August 2019


Atmospheric Chemistry and Physics Discussions

catalyse electron transfer reactions and formation of reactive oxygen species (ROS), which could pose oxidative stress in humans upon inhalation (Verma et al., 2015).

Biomass burning (BB) is considered as one of the main sources of HULIS in the atmosphere (Lin et al., 2010; Claeys et al., 2012; Pavlovic and Hopke, 2012; Zheng et al., 2013) and an important source of aerosol nitroaromatic compounds (NACs; Claeys et al., 2012; Song et al., 2018). Recent studies found that nitro-monoaromatic hydrocarbons (NMAHs), such as 4-nitrocatechol (4-NC; MW: 155 Da) and isomeric methyl-nitrocatechols (MNCs; MW: 169 Da) are abundant constituents of particulate matter (PM) HULIS, originating from BB (Claeys et al., 2012; Song et al., 2018).

NMAHs are emitted into the atmosphere by primary and secondary processes. 4-NC, MNCs, nitroguaiacols (NGs) and nitrosalicylic acids (NSAs) are predominantly formed by secondary oxidation of lignin thermal decomposition products (m-cresol, phenols, methoxyphenols, catechols, salicylic acid etc.) in the gas- and aqueous phase (Iinuma et al., 2010; Kelly et al., 2010; Kroflič et al., 2015; Frka et al., 2016; Teich et al., 2017; Finewax et al., 2018; Xie et al., 2017; Wang et al., 2019). Therefore, the yellow-coloured water-soluble 4-NC and MNCs have been proposed as suitable tracers for highly oxidized secondary BB aerosols (Iinuma et al., 2010; Kitanovski et al., 2012b; Kahnt et al., 2013; Caumo et al., 2016; Chow et al., 2016). In the past decade, the ambient PM nitrocatechols (NCs) have been measured in several studies world-wide, i.e. Europe (Iinuma et al., 2010; Zhang et al., 2010; Kitanovski et al., 2012b; Kahnt et al., 2013; Mohr et al., 2013; Teich et al., 2014; Frka et al., 2016), South America (Claeys et al., 2012; Caumo et al., 2016), North America (al Naiema and Stone, 2017), Asia (Chow et al., 2016; Li et al., 2016; Wang et al., 2019) and Australia (Iinuma et al., 2016). They represent a significant fraction of the PM organic carbon (OC), e.g. 0.8% in winter PM_{10} collected at an urban background location in Slovenia (range 0.4-1.3%; Kitanovski et al., 2012b), 0.75% in winter PM_{10} collected at rural site in Belgium (Kahnt et al., 2013) and ≈0.3% in PM_{10} collected in Brazil during the BB season (Caumo et al., 2016). Nitrosalicylic acids (2-hydroxy-nitrobenzoic acids) have been reported in PM samples collected at rural (van Pinxteren and Herrmann, 2007; van Pinxteren et al., 2012; Teich et al., 2017; Wang et al., 2018), urban (Kitanovski et al., 2012a and 2012b; Teich et al., 2017; Wang et al., 2018) and remote (Wang et al., 2018) sites. Similar to NCs, they are mainly associated with secondary BB aerosols (Kitanovski et al., 2012b; Teich at el., 2017; Wang et al., 2018). Nitrophenols (NPs), structurally related compounds to NCs, are emitted from primary sources (e.g. traffic, coal and wood combustion, industry and agricultural use of pesticides), which usually

https://doi.org/10.5194/acp-2019-673
Preprint. Discussion started: 7 August 2019


Atmospheric Chemistry and Physics Discussions

predominate their secondary formation, especially in urban areas (Harrison et al., 2005; Cecinato et al., 2005; Hoffmann et al., 2007; Iinuma et al., 2007; Zhang et al., 2010; Ganranoo et al., 2010; Özel et al., 2011; Mohr et al., 2013; Kitanovski et al., 2012a and 2012b; Inomata et al., 2015; Teich et al., 2017; Wang et al., 2018).

Polycyclic aromatic hydrocarbons (PAHs) and their nitrated and oxygenated derivatives (NPAHs and OPAHs), as well as hydroxy derivatives (OH-PAHs), are ubiquitous in the atmosphere (Walgraeve et al., 2010; Lammel, 2015; Bandowe and Meusel, 2017; Shahpoury et al., 2018). They are primarily emitted from incomplete combustion of fossil fuels (Zielinska et al., 2004; Karavalakis et al., 2010; Pham et al., 2013; Inomata et al., 2015), wood, coal and biomass burning (Ding et al., 2012; Shen et al., 2012, 2013a and 2013b; Huang et al., 2014; Vicente et al., 2016). The PAH derivatives are secondarily formed by the reaction of parent PAHs with atmospheric oxidants such as OH, NO_x and O_3. Some NPAHs have distinct sources; for instance, 3-nitrofluoranthene (3-NFLT) and 1-nitropyrene (1-NPYR) are specifically associated with combustion sources, whereas 2-nitrofluoranthene (2-NFLT) and 2-nitropyrene (2-NPYR) are produced through oxidation of their parent species in the atmosphere (Bandowe and Meusel, 2017). Similarly, OPAHs benzanthrone (OBAT), benz(a)fluorenone (BaOFLN) and benz(b)fluorenone (BbOFLN) have been associated with primary sources, whereas 9,10-anthraquinone (9,10-O_2ANT), 1,2-benzanthraquinone (1,2-O_2BAA), and 9-fluorenone (9-OFLN) have been attributed to both source types (Kojima et al., 2010; Souza et al., 2014; Lin et al., 2015; Zhuo et al., 2017). The primary sources dominate in winter time with residential heating surpassing traffic emission (Lin et al., 2015). It is anticipated that functionalized 2- and 3-ring PAHs (e.g. 2- and 3-ring OPAHs) would exhibit the highest hydrophilicity among their analogs and could also be part of PM HULIS (Vione et al., 2014; Fan et al., 2016; Haynes et al., 2019). The water-soluble OPAHs, in particular quinones, were suggested to contribute to light-absorption properties of brown carbon (Laskin et al., 2015; Haynes et al., 2019). Moreover, the ROS activity of HULIS from $PM_{2.5}$ was associated to OPAHs, i.e. quinones and hydroxy-quinones (Verma et al., 2015). It has been shown in controlled experiments that the chemical aging of PM from various origins would increase its ROS activity and this effect is enhanced in the presence of O_3 (Li et al., 2009; McWhinny et al., 2011; Stevanovic et al., 2013; Verma et al., 2014 and 2015; Antiñolo et al., 2015). This process has been attributed to oxidation of PAHs and formation of water-soluble derivatives.

https://doi.org/10.5194/acp-2019-673
Preprint. Discussion started: 7 August 2019

Atmospheric Chemistry and Physics Discussions

NMAHs, PAHs and N/OPAHs significantly contribute to the aerosol BrC due to their light-absorption capacity in the UV and visible range (Mohr et al., 2013; Teich et al., 2017; Xie et al., 2017). Determining the size-resolved mass distribution of the PM molecular tracers is important for assessing the particle emission sources, atmospheric transport, and health effects (Neusüss et al., 2000). In particular, there is a limited knowledge about the size-resolved characteristics of NMAHs and N/OPAHs, and their relation to atmospheric HULIS (Claeys et al., 2012; Song et al., 2018). Therefore, the aim of the present work is to fill this gap by studying the size-resolved PM from polluted urban air at two locations in central and southern Europe, i.e. Mainz (MZ), Germany and Thessaloniki (TK), Greece, and to apply these data to determine the possible emission sources. The concentrations of ions, organic acids, HULIS and HULIS-C in the samples used in this study can be found in a companion paper (Voliotis et al., 2017).

2. Experimental

2.1 Chemicals and solutions

Solvents including methanol (MeOH, Chromasolv, LC-MS grade; Fluka, Buchs, Switzerland), tetrahydrofuran (THF, LiChrosolv, HPLC grade; Merck, Darmstadt, Germany), high-purity water (18.2 MΩ cm; Elga PURELAB, Veolia Water Technologies, Celle, Germany), ethylenediaminetetraacetic acid (EDTA, trace metals basis; Sigma-Aldrich, St. Louis, USA), formic acid and ammonium formate (grade eluent additive for LC-MS; Fluka) were used for LC-MS mobile phase and sample preparation for NMAHs. Dichloromethane (DCM), *n*-hexane, and ethyl acetate (Suprasolv, GC-MS grade, Merck) were used for N/OPAH analysis. Analytical standards used in our study, their acronyms, and suppliers are listed in Tables 1 and S1. The internal standards (IS) of 2,4,6-trinitrophenol (picric acid, aqueous solution 1.0%; Sigma-Aldrich) and 4-nitrophenol-d_4 (4-NP-d4; LGC, Teddington, UK) were used for NMAH quantification, whereas 1-nitronaphthalene-d_7, 2-nitrofluorene-d_9, 9-nitroanthracene-d_9, 3-nitrofluoranthene-d_9, 1-nitropyrene-d_9, 6-nitrochrysene-d_{11}, 9,10-anthraquinone-d_8, and 9-fluorenone-d_8 (Chiron, Norway) were used for N/OPAH quantification. Individual stock solutions of NMAH standards were prepared in methanol at concentrations of 200 µg mL^{-1}, whereas those for N/OPAHs were prepared in toluene at 10 µg mL^{-1}. Standard mixtures were prepared for each substance class from individual stock solutions, and further used for preparation of calibration standards of NMAHs in methanol/water mixture (3/7, v/v) containing 5 mM ammonium formate buffer pH 3 and 400 µM

https://doi.org/10.5194/acp-2019-673
Preprint. Discussion started: 7 August 2019


Atmospheric Chemistry and Physics Discussions

EDTA (injection solvent), and calibration standards of N/OPAHs in ethyl acetate. NMAH and N/OPAH calibration standards were prepared in the concentration range of 0.1 to 500 and 0.25 to 1000 pg μL^{-1}, with a fixed IS concentration of 100 and 200 pg μL^{-1}, respectively.

2.2 Collection of samples

All PM samples were collected using a 5-stage high-volume cascade impactor with effective cut-off diameters: 0.49, 0.95, 1.5, 3 and 7.2 µm of aerodynamic particle size, D_p, and a backup filter collecting particles < 0.49 µm (Table 2). The sampling in MZ was done using a high-volume air sampler Baghirra HV-100P (Baghirra, Prague, Czech Republic) equipped with a multi-stage cascade impactor (Tisch Environmetal Inc., Cleves, USA, series 230, model 235) and a PM_{10} head. Downstream of the impactor, gaseous organics were collected in two polyurethane foam plugs (PUF; density 0.030 g cm^{-3}; Organika, Malbork, Poland) placed in a glass cartridge. The PM was sampled on slotted quartz fibre filters (QFFs, TE-230-QZ, Tisch Environmental Inc., 14.3×13.7 cm) and a QFF backup filter (Whatman, 20.3×25.4 cm). Four sets of samples were collected at MZ between November and December 2015, each over the period of 70 hrs (flow rate: 60 m^3 h^{-1}; Table 2). The impactor used in TK was a Sierra Instruments, model 235; the PM samples were collected on QFFs (Tisch Environmental TE-230QZ, slotted 5.7×5.7 cm) and on QFF backup filters (Pall, 2500 QAT-UP), without a PM_{10} head, as described in Voliotis et al. (2017).

2.3 Sample preparation and analytical methods

2.3.1 LC/MS analysis of nitro-monoaromatic hydrocarbons

Extraction of the filter samples for NMAH analysis was done using a validated procedure (Kitanovski et al., 2012b) with small modifications. Briefly, a 1.5 cm^2 section of the filter was spiked with both IS (spiked mass: 100 ng) and subsequently extracted three times (5 min each) with 10 mL methanolic solution of EDTA (3.4 nmol mL^{-1}) in an ultrasonic bath. The combined extracts were concentrated to 0.5 mL using a TurboVap II (bath temperature: 40°C, nitrogen gas pressure: 15 psi; Biotage, Uppsala, Sweden). The concentrated extract was filtered through a 0.2-µm PTFE syringe filter (4 mm, Whatman; GE Healthcare, Little Chalfont, UK) into a 2-mL vial and was evaporated to near dryness under the gentle stream of nitrogen (99.999%; Westfalen AG, Münster, Germany). Finally, the extract was dissolved in methanol/water mixture (3/7, *v*/*v*) containing 5 mM ammonium formate buffer pH 3 and 400 µM EDTA for LC/MS analysis.

https://doi.org/10.5194/acp-2019-673
Preprint. Discussion started: 7 August 2019

Atmospheric Chemistry and Physics Discussions

The NMAHs were determined using an Agilent 1200 Series HPLC system (Agilent Technologies, Waldbronn, Germany) coupled to an Agilent 6130B Series single quadrupole mass spectrometer equipped with an electrospray ionization (ESI) source. High-purity nitrogen was used as nebulizer and drying gas. The separation of the targeted analytes was done on an Atlantis T3 column (150 mm × 2.1 mm i.d., 3 µm particles size; Waters, Milford, USA), connected to an Atlantis T3 VanGuard pre-column (5 mm × 2.1 mm i.d., 3 µm particles size; Waters), using isocratic elution with a mobile phase consisted of MeOH/THF/water (30/15/55, *v*/*v*/*v*) mixture containing 5 mM ammonium formate buffer pH 3. The mobile phase flow rate, column temperature and injection volume were 0.2 mL min^{-1}, 30°C and 10 µL, respectively (Kitanovski et al., 2012b). The detection and quantification of NMAHs was done in single ion monitoring and negative ESI mode (Table 1). The optimized ESI-MS parameters were as follows: –1000V for the ESI capillary voltage, 30 psig for the nebulizer pressure and 12 L min^{-1} and 340°C for the drying gas flow and temperature, respectively. Due to the lack of a reference standard for 3-methyl-4-nitrocatechol (3-M-4-NC), its concentrations were calculated based on the calibration curve of 4-M-5-NC. This is justified based on the structural similarity of the two substances and therefore similar ionization efficiency under ESI-MS conditions. LC/MSD ChemStation (Agilent Technologies) was used for data acquisition and analysis.

2.3.2 Chemical analysis of nitro- and oxy-polycyclic aromatic hydrocarbons

N/OPAHs were extracted from PM samples following a QuEChERS method with slight modifications (Albinet et al., 2014; Shahpoury et al., 2018). Briefly, each filter paper was placed inside a glass centrifuge tube (Duran, Schott, Mainz, Germany) and spiked with a mixture of internal standards containing 60 ng of each 1-nitronaphthalene-d_7, 2-nitrofluorene-d_9, 9-nitroanthracene-d_9, 3-nitrofluoranthene-d_9, 1-nitropyrene-d_9, 6-nitrochrysene-d_{11}, 9,10-anthraquinone-d_8, and 9-fluorenone-d_8. 7 mL of DCM was then added to each tube, the tubes were capped and the samples were extracted by vortexing for 1.5 min. The extracts were passed through a glass funnel plugged with deactivated glass wool and concentrated to 0.5 mL using a TurboVap II. The concentrated extracts were loaded on pre-conditioned SiO_2 solid-phase extraction cartridges (500 mg; Macherey-Nagel, Weilmünster, Germany) and the target analytes were eluted with 9 mL of 65:35 *n*-hexane-DCM.

https://doi.org/10.5194/acp-2019-673
Preprint. Discussion started: 7 August 2019

Atmospheric Chemistry and Physics Discussions

The purified extracts containing the analytes were concentrated to 0.5 mL and the solvent was exchanged by adding 5 mL of ethyl acetate, concentrating the solution to 0.5 mL, and repeating the process three times. The sample volumes were adjusted to 0.3 mL and transferred to 2 mL vials containing 0.4 mL glass inserts. All solvents used for N/OPAH analysis were high-purity (Suprasolv, GC-MS; Merck, Darmstadt, Germany). All glassware used for analysis was pre-washed with lab-grade detergent, tap water and deionized water, and baked at 310°C for 12 hours. The samples were analysed using a Trace 1310 gas chromatograph (GC; Thermo Scientific, Waltham, MA, USA) interfaced to a TSQ8000 Evo triple-quadrupole mass selective detector (MS/MS; Thermo Scientific). The analysis was performed in negative chemical ionization with methane used as ionization gas (1.5 mL min^{-1} flow rate; > 99.99%; Messer, Bad Soden, Germany). The analytes were separated on a 30-m DB-5ms capillary column (0.25 mm ID, 0.25 µm film thickness; J&W, Santa Clara, CA, USA) with helium (99.99 %; Westfalen AG, Münster, Germany) as carrier gas at 1 mL min^{-1} flow rate. The GC inlet temperature was set to 250°C and operated in pulsed splitless mode (30 psi pulsed pressure for 1.5 min, and splitless time of 1.8 min). The GC oven temperature was held at 60°C for 2 min at the start of the analysis, then increased to 180°C at 15°C min^{-1}, and to 280°C at 5°C min^{-1}, followed by a final hold time of 15 min. MS transfer line and ion source temperature were set to 290 and 230°C, respectively. Emission current and electron energy were set to 100 µA and −70 eV, respectively. The target analytes were detected in selected ion monitoring mode, identified using their retention times and quantification ions (Table 1). The quantification was performed using the internal calibration method and 11-point calibration curves ranging from 0.25 to 1000 pg μL^{-1}. Trace Finder (Thermo Scientific, Waltham, USA) was used for chromatographic data acquisition and analysis.

2.3.3 Quality control and data analysis

Field blanks (n = 3) were prepared during sample collection by mounting the pre-baked filters on the sampler without switching it on. These filters were subsequently retrieved and processed along with the rest of the samples. Limits of quantification (LOQ) for analytes were calculated as mean concentration of each analyte in blanks + 3 standard deviations. When analyte concentrations in the samples exceeded the LOQ, mean blank concentrations were subtracted from those in the corresponding samples. Microsoft Office Excel 2013 (Microsoft Corp., Redmond, USA) and OriginPro 9.0 (OriginLab Corp., Northampton, USA) were used for statistical analysis and data

https://doi.org/10.5194/acp-2019-673
Preprint. Discussion started: 7 August 2019

Atmospheric Chemistry and Physics Discussions

visualization. Mass size distributions (MSDs) of NMAHs and N/OPAHs were additionally characterized by the mass median diameter (MMD), defined as log MMD = Σ (c_i log D_i)/ Σ c_i, with c_i and D_i being the concentration (ng m^{-3}) and geometric mean diameter, respectively, of six impactor stages. 0.001 µm was adopted as the lower cut-off of the lowermost stage (backup filter) and 10 µm as the upper cut-off of the uppermost stage, even in the absence of a PM_{10} head (i.e. TK samples).

3. Results and discussion

3.1 Levels of NMAHs

From the 11 targeted NMAHs, 8 were consistently detected in size-segregated PM from MZ and TK. 4-NG and DNOC were not detected in MZ samples, while being sporadically detected in the coarse PM (>3 µm) from TK. 2,4-DNP was detected more frequently in TK (three sample sets) than in MZ samples (one sample set).

The concentrations of NMAHs associated to PM_{10} (MZ) and total PM (TK) are given in Table S3. PM_{10} and total PM $\sum_{11}$NMAH concentrations in MZ and TK were 0.51-8.38 and 12.1-72.1 ng m^{-3}, respectively. In all sample sets, 4-NC was the most abundant NMAH with concentrations ranging within 0.05-3.90 ng m^{-3} (mean 2.46 ng m^{-3}; Table S3) in MZ samples, and 10 times higher concentrations in TK samples (5.89-36.33 ng m^{-3}; mean 22.11 ng m^{-3}; Table S3). Second most abundant NMAH in MZ was found to be 4-NP with concentrations between 0.24 and 1.27 ng m^{-3} (mean 0.83 ng m^{-3}; Table S3), while 4-M-5-NC was the second most abundant in TK samples (2.54 - 16.05 ng m^{-3}; mean: 9.79 ng m^{-3}; Table S3). In general, the concentration trends of NMAHs were 4-NC > MNCs > 4-NP > NPs > NSAs > DNP (dinitrophenols) for MZ samples, and 4-NC > MNCs > 4-NP > NSAs > NPs > DNP for TK samples. These trends are in good agreement with other studies, where 4-NC, MNCs and 4-NP were the most abundant NMAHs (Kitanovski et al., 2012b; Chow et al., 2016). However, we previously found different concentration trends in snow-scavenged atmospheric particles collected in MZ, where 4-NC and MNCs were the second most abundant NMAH species following NPs (Shahpoury et al., 2018). ∑NMAH winter concentrations at TK were higher than those found in winter $PM_{2.5}$ and PM_{10} from Hong Kong (China; Chow et al., 2016) and rural Belgium (Kahnt et al., 2013), respectively, but lower than NMAH concentrations in winter PM_{10} samples from Ljubljana (Slovenia; Kitanovski et al., 2012b) and Shanghai (China; Li et al., 2016). The concentrations of individual NMAHs in winter PM_{10} from

https://doi.org/10.5194/acp-2019-673
Preprint. Discussion started: 7 August 2019


Atmospheric Chemistry and Physics Discussions

MZ were among the lowest values reported so far (Iinuma et al., 2010; Kitanovski et al., 2012b; Kahnt et al., 2013; Mohr et al., 2013; Chow et al., 2016; Li et al., 2016; Teich et al., 2017; Wang et al., 2019).

In Table S3, one can easily notice the consistently higher (≈10 times) total PM concentrations of 4-NC, MNCs and NSAs in TK samples compared to those found in PM_{10} samples from MZ. Smaller concentration discrepancies among the sites were observed for 4-NP and methyl-nitrophenols (MNPs) (up to 3 times higher concentrations in TK samples). Since 4-NC, MNCs and NSAs are considered as suitable tracers for BB aerosols (Iinuma et al., 2010; Kitanovski et al., 2012b; Kahnt et al., 2013; Caumo et al., 2016; Chow et al., 2016; Teich et al., 2017), this suggests that the air masses over TK during sample collection were greatly influenced by BB emissions. To test this hypothesis, a correlation analysis was done for NMAHs. Except for NPs in TK samples, generally high correlations were observed within the NMAHs compound groups (NSAs, NCs, NPs; $R^2_{adj} > 0.8$; Table S4 and S5). The correlation analysis of TK samples showed several interesting features (Table S4). Firstly, 5-NSA highly correlated (R^2_{adj} 0.81 – 0.83) with 4-NP and potassium cation (K^+), but showed insignificant correlations with 4-NC, MNCs and nitrate. Moreover, 3-NSA showed significantly ($p<0.05$) high correlation only with K^+, but moderate with 4-NP. Additionally, 4-NP was highly correlated with K^+ and nitrate (R^2_{adj} 0.94 and 0.81, respectively). Secondly, 4-NC and 4-M-5-NC showed low correlations with K^+ and nitrate, but highly correlated with 3-M-4-NP (R^2_{adj} 0.74 and 0.78, respectively). In our previous work (Kitanovski et al., 2012b), high correlations between NSAs and 4-NC, MNCs or nitrates were observed ($R^2_{adj} > 0.8$), supporting NSAs' secondary origin (Kitanovski et al., 2012b; Teich et al., 2017). Our TK results indicate different emission sources between NSAs and 4-NP on the one hand, and 4-NC and MNCs on the other hand. 5-NSA and 4-NP (2-M-4-NP included) most likely had the same emission source, i.e. BB (both correlate with K^+), and were probably formed by aqueous-phase nitration of their phenolic precursors (especially for 4-NP and 2-M-4-NP, which both highly correlated with nitrates) in deliquescent aerosol (Kroflič et al., 2018). Additionally, 3-NSA (insignificantly correlated with nitrate) was probably emitted primarily by BB (Wang et al., 2017). In contrast, low correlations of 4-NC and MNCs with K^+ and nitrates suggest that BB and aqueous-phase nitration might not be the dominating emission sources, and that their possible main source could be gas-phase nitration of anthropogenic precursors (Finewax et al., 2018), such as benzene and toluene (Xie et al., 2017; Wang et al., 2019), emitted from fossil fuel combustion (e.g. traffic, coal

https://doi.org/10.5194/acp-2019-673
Preprint. Discussion started: 7 August 2019


Atmospheric Chemistry and Physics Discussions

combustion). The statistically significant ($p<0.05$) correlations of 3-M-4-NP with 4-NC and 4-M-5-NC, in contrast to the correlations with 4-NP and nitrates, suggest that most likely 3-M-4-NP had similar emission sources with NCs (i.e. fossil fuel combustion). It can be noted from Table S4 that MNP isomers (2-M-4-NP and 3-M-4-NP) probably had different main emission sources, i.e. aqueous-phase nitration of a 2-M-4-NP precursor emitted from BB *vs.* fossil fuel combustion in case of 3-M-4-NP (Noguchi et al., 2007).

Correlation analysis for NMAHs in MZ samples presents quite a different picture (Table S5). Statistically significant ($p<0.05$) high correlations were observed among different NMAH compound groups (i.e. NSAs, NCs, NPs), with most of R^2_{adj} higher than 0.8. K^+ was correlated with 5-NSA, 4-NC, MNCs and 3-M-4-NP, indicating their predominant emission from BB. Nitrate showed high correlations ($R^2_{adj}>0.9$) with 3-NSA, 4-NP, 2-M-4-NP and 2,4-DNP, suggesting that aqueous-phase nitration was a main source for these compounds over MZ (Table S5). Two pairs of positional isomers i.e. 3-NSA/5-NSA and 2-M-4-NP/3-M-4-NP showed distinct correlations within their pair with regard to nitrate and K^+. 3-NSA and 2-M-4-NP, which were highly correlated with nitrates, showed no correlation with K^+, indicating that aqueous-phase chemistry could have played a significant role in their formation. In contrast, the opposite was observed for 5-NSA and 3-M-4-NP (Table S5). In summer $PM_{2.5}$ over a rural site in northern China, Wang et al. (2018) observed weak correlations of NSAs with NO_2 that could indicate formation processes other than nitration. Primary NSA emission from traffic or BB cannot be excluded, since their positional isomers were found in diesel exhaust particles (Seki et al., 2010) or in BB smoke particles (Wang et al., 2017). The correlations of 4-NC and MNCs with K^+, 4-NP and MNPs suggest similar sources for NCs and NPs over MZ (Chow et al., 2016; Voliotis et al., 2017; Wang et al., 2018).

3.2 Mass size distributions of NMAHs

MSDs of NMAHs over the two sampling locations are given in Fig. 1 and 2. NSAs (3-NSA and 5-NSA) and NCs (4-NC, 4-M-5-NC, 3-M-5-NC and 3-M-4-NC) showed unimodal distributions with MSDs generally peaking in the finest PM fraction ($PM_{0.49}$) in both MZ and TK samples. Overall, NMAHs were prominent in smaller size fractions ($PM_{0.95}$) in MZ compared to TK (Fig. 1 and 2). For NSAs, in one out of the four samples collected at MZ, MSDs peaked in $PM_{1.5-0.95}$ fraction, while the $PM_{0.95}$ mass fractions of 3-NSA and 5-NSA were 22% and 44%, respectively (Fig. S1a). In this sample only, 5-NSA showed bimodal distribution (dominant peaks in $PM_{0.49}$ and $PM_{1.5-0.95}$).

https://doi.org/10.5194/acp-2019-673
Preprint. Discussion started: 7 August 2019


Atmospheric Chemistry and Physics Discussions

Moreover, 4-NP and MNPs were the most abundant NMAHs (Fig.S1a). The dominant MSD peak of NSAs in $PM_{1.5-0.95}$ and the concentration abundance of 4-NP and MNPs could indicate possible influence of primary traffic emissions (fossil fuel combustion; Seki et al., 2010; Inomata et al., 2015) at the beginning of the sampling campaign in MZ. During the next sampling periods at MZ site (Figs. S1b, S1c and S1d), 75-86% of NSAs' PM_{10} mass was associated with $PM_{0.95}$, which is in line with the observations at TK (66-82% of total PM mass belongs to $PM_{0.95}$; Fig. S2). At both sites, usually more than 90% of the compound total mass was associated with PM_3 (range: 83-99%). 87-93% and 82-88% of NCs at MZ and TK were associated with $PM_{0.95}$ (Figs. S1, S2 and S5). The coarse mode (>3 μm) accounted for only 1% (MZ) or 2.5% (TK). The larger coarse fraction found in TK could be partially attributed to the fact that the sampling system did not have a PM_{10} inlet, thus it could potentially collect coarse particles up to approximately 30 μm (Voliotis et al., 2017). The unimodal distributions of NCs peaking in the fine PM fraction are in line with the only report on MSDs of 4-NC (Li et al., 2016). The MSDs of HULIS in MZ and TK closely followed the MSDs of NCs and NSAs (Figs. 1 and 2), suggesting that these compounds could be important constituents of PM HULIS (for detailed discussion see Sect. 3.5). The accumulation of the NCs' and NSAs' mass in the submicrometer (<0.95 μm) PM fractions could indicate fresh combustion emissions (e.g. BB) and/or gas-to-particle conversion processes of their precursors over MZ and TK (Li et al., 2016).

Nitrophenols (i.e. 4-NP, 2-M-4-NP and 3-M-4-NP) showed bimodal distributions with a dominant peak in the finest fraction ($PM_{0.49}$) and a smaller peak in $PM_{3-0.95}$ (Figs. 1, 2, S1, S2 and S5). Bimodal distribution of NPs (i.e. 4-NP, 4-NG, 2,6-dimethyl-4-nitrophenol and 2,6-dinitrophenol) with a small mode peak in the fine PM fraction and a big one in the coarse fraction, was recently reported during winter haze episodes over Shanghai, China (Li et al., 2016). Our results imply that BB and gas-to-particle conversion processes were likely more prevalent emission sources for NPs in MZ and TK (dominant NPs' peak in $PM_{0.49}$) than fossil fuel (diesel) combustion sources (Harrison et al., 2005; Noguchi et al., 2007; Inomata et al., 2015; Li et al., 2016). For 4-NP, at both sites, around 80% of PM_{10} mass (or of the total PM mass at TK) was associated with PM_3, while ≈ 60% was associated with $PM_{0.95}$ (Figs. S1 and S2). Similarly, for methyl-nitrophenols 83-88% of PM_{10} mass at MZ and 75-83% of total PM mass at TK sites were associated with PM_3, while 58-65% of PM_{10} at MZ and 48-61% of total PM mass at TK sites were associated with $PM_{0.95}$ (Figs. S1 and S2).

https://doi.org/10.5194/acp-2019-673
Preprint. Discussion started: 7 August 2019


Atmospheric Chemistry and Physics Discussions

MMD of NMAHs was 0.10 µm (0.24 for NPs, 0.07 for NCs and 0.11 µm for NSAs) at MZ *vs*. 0.27 µm (0.60 for NPs, 0.24 for NCs and 0.31 µm for NSAs) at TK. The larger MMDs at TK could be explained by the larger size range collected at this site as mentioned above, but they could also be indicative of aerosol aging. In aged aerosols, semivolatiles are expected to be re-distributed with the MMD approaching the surface mean diameter, which for urban and continental aerosol peaks around 0.2 µm (Jaenicke, 1988), a shift which could not be resolved by the sampling technique applied. Note that the low size resolution (6 stages) may hide modes, which in particular applies for the so-called accumulation mode, which adds mostly to $PM_{0.49}$, but also to the size fraction between 0.49 and 0.95 µm.

3.3 Levels of N/OPAHs

N/OPAHs were studied in size-resolved PM in both MZ and TK sites. At both sites, particle-phase OPAHs were detected more frequently than NPAHs: seven out of eight OPAHs targeted for analysis were detected in nearly all MZ and TK samples (Table S3; Figs. S3 and S4). In contrast, only eight out of seventeen targeted NPAHs were found in the PM samples, of which only 1-nitronaphthalene (1-NNAP), 9-nitroanthracene (9-NANT), 2-NFLT, and 7-nitrobenz(*a*)anthracene (7-NBAA) were detected in both MZ and TK samples. Interestingly, 3-nitrophenanthrene (3-NPHE), 3-NFLT, and 1- and 2-NPYR were only found in TK samples. This was not due to differences in individual LOQs between the two sites (see Table S2). The mean concentrations of NPAHs in PM were dominated by 9-NANT followed by 2-NFLT and 7-NBAA at both sites (Figs. 1 and 2, Table S3), with concentrations reaching to 225, 154, and 71 pg m^{-3}, respectively. This pattern closely resembles those previously reported for PM from several locations in central Europe (Tomaz et al., 2016, and references therein), including NPAHs found in snow-scavenged atmospheric particles from MZ sample site (Shahpoury et al., 2018). As for OPAHs, the mean analyte concentrations in PM were dominated by OBAT, followed closely by BbOFLN, BaOFLN, 9,10-O_2ANT, and 1,2-O_2BAA. The latter two quinones could be of high importance due to their redox activity, and their potential to catalyse the formation of reactive oxygen species (ROS) within the human respiratory system (Ayres et al., 2008; Bates et al., 2019). The two substances were found to dominate two out of four MZ samples with concentrations up to 221 and 137 pg m^{-3}, respectively. These concentrations were higher at TK site and reached 354 and 514 pg m^{-3}, respectively.

https://doi.org/10.5194/acp-2019-673
Preprint. Discussion started: 7 August 2019


Atmospheric Chemistry and Physics Discussions

Overall, all N/OPAHs showed considerably higher concentrations in TK than in MZ samples. ∑NPAH concentrations in PM_{10} from MZ and in total PM from TK were <LOQ-90 and 76-578 pg m^{-3}, respectively, whereas ∑OPAHs demonstrated much higher levels ranging 47-1636 and 858-4306 pg m^{-3}, respectively. The sum of three quinones 1,4-naphthoquinone (1,4-O_2NAP), 9,10-O_2ANT, and 1,2-O_2BAA were 30-363 and 428-873 pg m^{-3}, respectively. The levels of particle-phase NPAHs found in MZ fall in the lower end of the range (50-500 pg m^{-3}) observed for various types of sites in Europe (Tomaz et al., 2016, and references therein). The levels at TK represent the upper end of this range, while being within the concentration range previously found at other sites in Thessaloniki (1204 ± 249 pg m^{-3} at a traffic site, 383 ± 77 pg m^{-3} at an urban background site, Besis et al., 2017). The total OPAH concentrations at both sites fall in the lower end of the range previously observed in Europe (0.5-50 ng m^{-3}; Tomaz et al., 2016 and references therein).

N/OPAHs were predominant in the sub-micrometre PM fraction ($PM_{0.95}$; 85-91% of PM_{10} at MZ and 78-85% of total PM at TK site; Figs. 1, 2, S3, S4 and S5), with relatively more enrichment in $PM_{0.49}$ compared to $PM_{0.49-0.95}$ across the two sites. The mean concentrations of ∑NPAHs in $PM_{0.49}$ from MZ and TK were 101±73 and 417±134 pg m^{-3}, whereas in $PM_{0.49-0.95}$ were 22.8±15.9 and 222±95 pg m^{-3}, respectively. ∑OPAHs showed similar patterns at MZ and TK sites – they were 460±566 and 1426±1210 pg m^{-3} in $PM_{0.49}$, respectively, and 81.6±78.8 and 555±209 pg m^{-3} in $PM_{0.49-0.95}$. The targeted NPAHs did not show a second mode in any sample, whereas for 9-OFLN and 9,10-O_2ANT a second mode was found in MZ samples. Such differences between mass distributions indicate that these OPAHs are subject to different atmospheric processes compared to the other N/OPAHs that we studied. This could point at different emission and formation pathways in the atmosphere (see Sect. 3.4 for further discussion). Some of the OPAHs with single O-atom, namely OBAT, BaOFLN, and BbOFLN, originate from primary sources (i.e. combustion of fossil fuels and biomass; Albinet et al., 2007; Karavalakis et al., 2010; Shen et al., 2013b; Souza et al., 2014; Huang et al., 2014; Tomaz et al., 2016; Vicente et al., 2016), whereas some quinones, such as 9,10-O_2ANT and 1,2-O_2BAA, are associated with both primary and secondary sources (Kojima et al., 2010; Souza et al., 2014; Lin et al., 2015; Zhuo et al., 2017). In order to better understand the potential sources of the target substances, we performed correlation analysis between the measured levels of N/OPAHs and other PM constituents, namely, WSOC, HULIS, nitrate, sulphate, and K^+. We found a significant correlation (n = 5, $p<0.05$) between 9,10-O_2ANT and 1,2-O_2BAA at TK site, which suggests a common emission source (Table S6). The data shown in

https://doi.org/10.5194/acp-2019-673
Preprint. Discussion started: 7 August 2019


Atmospheric Chemistry and Physics Discussions

412 Tables S6 and S7 also indicate significant correlations ($p<0.05$) between the levels of BaOFLN
413 and 1-NPYR (produced by primary sources), and WSOC, HULIS, and K^+ (BB marker) in TK
414 samples. 1-NPYR is the predominant congener among NPAHs found in diesel engine exhaust
415 particles and was proposed as marker for diesel emission (Bamford et al., 2003; IARC 2013), but
416 it may also be emitted with relatively small quantities from biomass-fuelled combustion (Shen et
417 al., 2012; Orakij et al., 2017). These findings suggest the importance of primary emission sources
418 including BB and diesel exhaust in TK study area. For MZ samples, we found significant
419 correlations ($n = 4$, $p<0.05$) of 9-OFLN, BaOFLN, and 9-NANT with WSOC and HULIS, without
420 any significant correlations to K^+, suggesting the presence of mixed air masses that were fed by
421 both primary and secondary sources at MZ site. The absence of both NPYR isomers in MZ samples,
422 which are indicative of road traffic and industrial emissions and long-range transported pollution
423 (IARC, 1989; Finlayson-Pitts and Pitts, 2000; Lammel et al., 2017), indicates that chemically aged
424 air was advected during the MZ campaign (Voliotis et al., 2017).
425
426 **3.4 Mass size distribution of N/OPAHs**
427 N/OPAH MSDs are shown in Figs. 1 and 2. On average, the MMDs of NPAHs were 0.06 µm at
428 MZ and 0.12 µm at TK, while those for OPAHs were 0.06 µm at MZ and 0.10 µm at TK. The
429 MMDs for quinones were 0.07 and 0.15 at the two sites, respectively. We found two distinct MSD
430 patterns among the samples: the first pattern observed in three samples across the two sites (one
431 sample set from MZ and two sets from TK; Figs. S3c, S4a, d and e), was dominated by OBAT
432 followed by BbOFLN. The MMD of OPAHs in these three samples was on average 0.06 µm
433 (ranging within 0.05-0.09 µm). The unique analyte distribution in these samples was accompanied
434 by a noticeably higher enrichment in $PM_{0.49}$ as well as relatively high concentrations compared to
435 the rest of samples. The preferential enrichment of OBAT, BaOFLN, and BbOFLN in sub-
436 micrometre PM was previously reported from locations in Europe, Asia, and the USA (Allen et al.,
437 1997; Albinet et al., 2008; Ladji et al., 2009; Ringuet et al., 2012; Shen et al., 2016; Gao et al.,
438 2019). The observed pattern could be the evidence of fresh emission from primary sources, as was
439 discussed in the previous section. The second pattern, which was seen in the remaining six sample
440 sets, was considerably different: the target substances were more evenly distributed across different
441 PM size ranges, and often dominated by relatively high abundance of quinones, 9,10-O_2ANT and
442 1,2-O_2BAA – the two quinones were previously reported with preferential enrichment in ultrafine

https://doi.org/10.5194/acp-2019-673
Preprint. Discussion started: 7 August 2019


Atmospheric Chemistry and Physics Discussions

PM (Ringuet et al., 2012; Shen et al., 2016). The MMD of OPAHs in these five sample sets was on average 0.25 µm (ranging within 0.08-0.49 µm). This distribution points at relatively aged air masses and the contribution of both primary and secondary sources.

In terms of the inter-site variability of target substance MSD, the size fraction $PM_{0.49}$ was more prominent in MZ than in TK, i.e. on average 74% for NPAHs, 75% for OPAHs, 69% for quinones at MZ, compared to 55, 60, and 52%, respectively, at TK site (Figs. 1-2 and S3-5). The largest differences found among each substance group were for 9-NANT (28% higher at MZ), BbOFLN (25% higher), and 1,2-O_2BAA (17% higher). The values for NPAHs from TK were lower than those previously found for wintertime PM at this site (59 and 71% for a traffic and urban background site, respectively; Besis et al., 2017). The higher enrichment of predominant NPAHs (9-NANT and 2-NFLT; Figure S3-S4) in $PM_{0.49}$ in the present study is in agreement with the MSDs reported for these compounds from several other locations in Europe and Asia (Ringuet et al., 2012; Lan et al., 2014; Lammel et al., 2017). The preferential enrichment of N/OPAHs in sub-micron PM, especially $PM_{0.49}$, raises concerns with respect to the inhalation toxicity of airborne PM; this is because $PM_{0.49}$ is capable of reaching deeper regions in the lung. This is exacerbated by the ability of quinones to catalyse redox reactions and the formation of ROS in the respiratory system.

3.5 NMAHs and N/OPAHs as part of HULIS

Because of their water-solubility, NMAHs are constituents of PM HULIS and WSOC (Claeys et al., 2012; Teich et al., 2017). This substance class contributed ≈0.4 and 1.8% to HULIS mass at the MZ and TK sites, respectively (Table 3). This contribution was fairly even across the size fractions addressed, while showing a maximum for particles size 0.95-3 µm, namely ≈0.7 and 2.0% by mass at the MZ and TK sites, respectively. The large particle size, 0.95-3 µm, points to the significance of aqueous phase processes and in general slower formation of NMAHs (Voliotis et al., 2017). The water-soluble N/OPAHs, i.e. 1,4-O_2NAP and 1-NNAP, contributed up to 0.0006 % to HULIS (Table 3; water solubility of ≥50 mg L^{-1} was used as criterion), with values peaking in the PM size fractions 0.95-3 and >3 µm at MZ and TK, respectively. Similar to NMAHs, the N/OPAH mass mixing ratios in HULIS did not significantly vary with particle size (Table 3).

Our reported NMAH contribution to HULIS mass is in good agreement with the results of previous reports from urban sites in Europe (Kitanovski et al., 2012b; Claeys et al., 2012) and Brazil (Caumo et al., 2016). Specifically, Kitanovski et al. (2012) found that NMAHs contributed 0.4-1.3% to the

https://doi.org/10.5194/acp-2019-673
Preprint. Discussion started: 7 August 2019


Atmospheric Chemistry and Physics Discussions

474 winter urban PM_{10} OC mass from Ljubljana (Slovenia), while in another study, 4-NC alone
475 contributed 0.46% and 0.04% to the HULIS mass in urban spring and summer $PM_{2.5}$ from Budapest
476 (Hungary), respectively (Claeys et al., 2012). Moreover, NMAHs (4-NP, 4-NC, MNCs and
477 dimethyl-nitrocatechols (DMNCs)) contributed 0.28% and 0.35% to the OC mass in winter PM_{10}
478 samples from São Paulo, Brazil (Caumo et al., 2016). Lower NMAH contribution to HULIS (or
479 OC) mass were reported for rural sites in Europe. For example, 4-NC contributed 0.03% to the
480 HULIS mass in summer $PM_{2.5}$ from K-puszta, Hungary (Claeys et al., 2012), while total NMAHs
481 (NPs, 4-NC, MNCs and DMNCs) presented 0.75% of OC mass in winter PM_{10} sampled at a rural
482 background site in Belgium (Kahnt et al., 2013).
483 In Sect. 3.2 we emphasized the similar MSDs at both locations between HULIS on one side and
484 NCs and NSAs on the other. These two NMAH subclasses on average contributed to ≈83% and
485 ≈94% of total NMAHs in $PM_{0.95}$, and ≈55% and 87% of total NMAHs in $PM_{3\text{-}0.95}$ at MZ and TK
486 sites, respectively (Table S8). At both sites, NCs were the dominant NMAH species. It is also
487 interesting to note that HULIS showed higher correlations with NSAs and NCs in MZ (R^2_{adj} 0.68-
488 0.98; Table S5), than in TK (R^2_{adj} 0.24-0.59; Table S4). BaOFLN and 1-NPYR, as well as 9-OFLN,
489 BaOFLN and 9-NANT showed similar MSDs and significant correlations ($R^2_{adj} \geq 0.8$; Tables S6-
490 S7) with HULIS at TK and MZ, respectively, suggesting that these N/OPAHs are most likely
491 constituents of the HULIS. The significant correlations in the levels of 1-NPYR with HULIS,
492 WSOC, and K^+ (Table S6) are particularly interesting, as 1-NPYR is exclusively associated with
493 primary emission sources. These observations are in line with our previous discussion that MZ site
494 was mainly influenced by aged air masses, while TK site by a mixture of fresh (BB and fossil fuel)
495 emissions and aged aerosols (Voliotis et al., 2017).
496 With mass mixing ratios of the order of 1%, NMAHs are constituents of HULIS with limited
497 significance by mass, but their relevance is more significant due to their optical properties (Mohr
498 et al., 2013; Laskin et al., 2015; Teich et al., 2017; Xie et al., 2017). Teich et al. (2017) found that
499 the mass contributions of total NMAHs (NPs and NSAs) to WSOC on average was five times lower
500 than their contribution to the light absorption of the aqueous PM extract at 370 nm (Teich et al.,
501 2017). This implies that even small fractions of chromophoric HULIS compounds such as NMAHs
502 and water soluble N/OPAHs can have an excessive influence on the aerosol light absorption (Mohr
503 et al., 2013; Teich et al., 2017) and the atmospheric photochemical processes, especially in polluted
504 areas (Laskin et al., 2015; Teich et al., 2017).

https://doi.org/10.5194/acp-2019-673
Preprint. Discussion started: 7 August 2019

Atmospheric Chemistry and Physics Discussions

4. Final remarks

We studied the composition and MSDs of NMAHs and N/OPAHs in PM from urban locations in Germany and Greece, with some of the target substances (i.e. NSAs, MNCs and MNPs) studied in size-resolved PM for the first time. At both locations, NCs were the most abundant NMAH species, and OPAHs were more abundant and more frequently detected than NPAHs. The total concentrations of the most abundant NMAHs, NCs, and N/OPAHs were up to 10 times higher in TK than in MZ. Correlation analysis of NMAHs revealed distinct features among the sites, suggesting mixed air masses influenced by fresh BB and aged fossil fuel combustion emissions at TK, and aged advected air influenced by combustion emissions (i.e. BB) at MZ.

The MSDs of NMAHs, OPAHs and NPAHs were rather similar, but exhibited temporal and spatial variations due to daily changes in atmospheric conditions and different sources. In general, NCs, NSAs, OPAHs and NPAHs showed unimodal MSDs peaking in the finest PM fraction, $PM_{0.49}$, which was more prominent in MZ than in TK. NPs exhibited bimodal MSDs with the dominant peak in $PM_{0.49}$. The MMDs of all chemical classes were lower at MZ than at TK. Larger MMDs at TK could be explained by the larger PM size range collected at this site, but they could also be an indication of aerosol aging. On average, NMAHs and water-soluble N/OPAHs (i.e. 1,4-O_2NAP and 1-NNAP) contributed up to 1.8 and 0.0006% to the HULIS mass in the study areas. Although NMAHs and N/OPAHs represent a small fraction of PM HULIS (and WSOC), due to their light absorption properties, their impact on the total aerosol light absorption could be disproportionally large. This is particularly important for atmospheric photochemical processes in polluted areas.

Acknowledgements

We thank Eleni Papakosta (Prefecture of Thessaloniki), Thorsten Hoffmann and Anna Honcza (Max Planck Institute for Chemistry) for onsite and laboratory support. This research was supported by the Max Planck Society and the Postgraduate Program “Environmental Chemistry and Pollution Control” of the Aristotle University of Thessaloniki.

Author contributions. GL and CS conceived the study. PS and AV conducted the air sampling and field measurements. ZK and PS did the chemical analysis of samples. ZK, PS, and GL did the data analysis. ZK, PS, and GL discussed the results and wrote the manuscript with input from all co-authors.

https://doi.org/10.5194/acp-2019-673
Preprint. Discussion started: 7 August 2019

Atmospheric Chemistry and Physics Discussions

References

Albinet, A., Leoz-Garziandia, E., Budzinski, H. and Villenave, E.: Polycyclic aromatic hydrocarbons (PAHs), nitrated PAHs and oxygenated PAHs in ambient air of the Marseilles area (South of France): concentrations and sources, Sci. Total Environ., 384, 280–292, doi:10.1016/j.scitotenv.2007.04.028, 2007.

Albinet, A., Leoz-Garziandia, E., Budzinski, H., Villenave, E. and Jaffrezo, J.-L.: Nitrated and oxygenated derivatives of polycyclic aromatic hydrocarbons in the ambient air of two French alpine valleys Part 2: particle size distribution, Atmos. Environ., 42, 55–64, doi:10.1016/j.atmosenv.2007.10.008, 2008.

Albinet, A., Nalin, F., Tomaz, S., Beaumont, J. and Lestremau, F.: A simple QuEChERS-like extraction approach for molecular chemical characterization of organic aerosols: application to nitrated and oxygenated PAH derivatives (NPAH and OPAH) quantified by GC–NICIMS, Anal. Bioanal. Chem., 406, 3131–3148, doi:10.1007/s00216-014-7760-5, 2014.

Allen, J.O., Dookeran, N.M., Taghizadeh, K., Lafleur, K.L., Smitz, K.A. and Sarofim, A.F.: Measurement of oxygenated polycyclic aromatic hydrocarbons associated with a size-segregated urban aerosol. Environ. Sci. Technol., 31, 2064-2070, doi:10.1021/es960894g, 1997.

al Naiema, I.M. and Stone, E.A.: Evaluation of anthropogenic secondary organic aerosol tracers from aromatic hydrocarbons, Atmos. Chem. Phys., 17, 2053–2065, doi:10.5194/acp-17-2053-2017, 2017.

Andreae, M.O. and Gelencser, A.: Black carbon or brown carbon? The nature of light-absorbing carbonaceous aerosols. Atmos. Chem. Phys., 6, 3131-3148, doi:10.5194/acp-6-3131-2006, 2006.

Antiñolo, M., Willis, M. D., Zhou, S. and Abbatt, J. P. D.: Connecting the oxidation of soot to its redox cycling abilities, Nat. Commun., 6, 6812, doi:10.1038/ncomms7812, 2015.

Ayres, J. G., Borm, P., Cassee, F. R., Castranova, V., Donaldson, K., Ghio, A., Harrison, R. M., Hider, R., Kelly, F., Kooter, I. M., Marano, F., Maynard, R. L., Mudway, I., Nel, A., Sioutas, C., Smith, S., Baeza-Squiban, A., Cho, A., Duggan, S. and Froines, J.: Evaluating the toxicity of airborne particulate matter and nanoparticles by measuring oxidative stress potential – a workshop report and consensus statement, Inhal. Toxicol., 20, 75–99, doi:10.1080/08958370701665517, 2008.

Bamford, H. A., Bezabeh, D. Z., Schantz, M. M., Wise, S. A. and Baker, J. E.: Determination and comparison of nitrated-polycyclic aromatic hydrocarbons measured in air and diesel particulate reference materials, Chemosphere, 50, 575–587, doi:10.1016/S0045-6535(02)00667-7, 2003.

Bandowe, B. A. M. and Meusel, H.: Nitrated polycyclic aromatic hydrocarbons (nitro-PAHs) in the environment – a review, Sci. Total Environ., 581–582, 237–257, doi:10.1016/j.scitotenv.2016.12.115, 2017.

Bates, J. T., Fang, T., Verma, V., Zeng, L., Weber, R. J., Tolbert, P. E., Abrams, J. Y., Sarnat, S. E., Klein, M., Mulholland, J. A. and Russell, A. G.: Review of acellular assays of ambient particulate matter oxidative potential: methods and relationships with composition, sources, and health effects, Environ. Sci. Technol., 53, 4003–4019, doi:10.1021/acs.est.8b03430, 2019.

Besis, A., Tsolakidou, A., Balla, D., Samara, C., Voutsa, D., Pantazaki, A., Choli-Papadopoulou, T. and Lialiaris, T. S.: Toxic organic substances and marker compounds in size-segregated urban particulate matter - implications for involvement in the in vitro bioactivity of the extractable organic matter, Environ. Pollut., 230, 758–774, doi:10.1016/j.envpol.2017.06.096, 2017.

Caumo, S.E.S., Claeys M., Maenhaut W., Vermeylen, R., Shabnam B., Shalamzari, M.S. and Vasconcellos, P.C.: Physicochemical characterization of winter PM_{10} aerosol impacted by sugarcane burning from São Paulo city, Atmos. Environ., 145, 272–279, doi:10.1016/j.atmosenv.2016.09.046, 2016.

Cecinato, A., di Palo, V., Pomata, D., Scianò, M.C.T. and Possanzini, M.: Measurement of phase-distributed nitrophenols in Rome ambient air, Chemosphere, 59, 679–683. doi:10.1016/j.chemosphere.2004.10.045, 2005.

Chow, K.S., Hilda, X.H.H. and Yu, J.Z.: Quantification of nitroaromatic compounds in atmospheric fine particulate matter in Hong Kong over 3 years: field measurement evidence for secondary formation derived from biomass burning emissions, Environ. Chem., 13, 665–673, doi:10.1071/EN15174, 2016.

https://doi.org/10.5194/acp-2019-673
Preprint. Discussion started: 7 August 2019

Atmospheric Chemistry and Physics Discussions

582 Claeys, M., Vermeylen, R., Yasmeen, F., Gómez-González, Y., Chi, X., Maenhaut, W., Mészáros, T. and Salma, I.:
583 Chemical characterisation of humic-like substances from urban, rural and tropical biomass burning environments using
584 liquid chromatography with UV/vis photodiode array detection and electrospray ionisation mass spectrometry.
585 Environ. Chem., 9, 273–284, doi:10.1071/EN11163, 2012.

586 Decesari, S., Facchini, M.C., Fuzzi, S. and Tagliavini E.: Characterization of water-soluble organic compounds in
587 atmospheric aerosol: a new approach, J. Geophys. Res., 105, 1481–1489, doi:10.1029/1999JD900950. 2000.

588 Ding, J., Zhong, J., Yang, Y., Li, B., Shen, G., Su, Y., Wang, C., Li, W., Shen, H., Wang, B., Wang, R., Huang, Y.,
589 Zhang, Y., Cao, H., Zhu, Y., Simonich, S. L. M. and Tao, S.: Occurrence and exposure to polycyclic aromatic
590 hydrocarbons and their derivatives in a rural Chinese home through biomass fuelled cooking, Environ. Pollut., 169,
591 160–166, doi:10.1016/j.envpol.2011.10.008, 2012.

592 Duarte, R.M.B.O, Pio, C.A. and Duarte, A.C.: Spectroscopic study of the water-soluble organic matter isolated from
593 atmospheric aerosols collected under different atmospheric conditions, Anal. Chim. Acta, 530, 7–14,
594 doi:10.1016/j.aca.2004.08.049, 2005.

595 Fan, X., Wei, S., Zhu, M., Song, J. and Peng, P.: Comprehensive characterization of humic-like substances in smoke
596 PM2.5 emitted from the combustion of biomass materials and fossil fuels, Atmos. Chem. Phys., doi:10.5194/acp-16-
597 13321-2016, 2016.

598 Finewax, Z., de Gouw, J.A. and Ziemann, P.J.: Identification and quantification of 4-nitrocatechol formed from OH
599 and NO_3 radical-initiated reactions of catechol in air in the presence of NO_x: implications for secondary organic aerosol
600 formation from biomass burning. Environ. Sci. Technol., 52, 1981-1988, doi:10.1021/acs.est.7b05864, 2018.

601 Finlayson-Pitts, B.J. and Pitts, J.N.: Chemistry of the Upper and Lower Atmosphere: Theory, Experiments,
602 Application, San Diego, Academic Press, USA, 2000.

603 Frka, S., Šala, M., Kroflič, A., Huš, M., Čusak, A. and Grgić, I., Quantum chemical calculations resolved identification
604 of methylnitrocatechols in atmospheric aerosols, Environ. Sci. Technol., 50, 5526–5535, doi:10.1021/acs.est.6b00823,
605 2016.

606 Ganranoo, L., Mishra, S.K., Azad, A.K., Shigihara, A., Dasgupta, P.K., Breitbach, Z.S., Armstrong, D.W., Grudpan,
607 K. and Rappenglück, B.: Measurement of nitrophenols in rain and air by two-dimensional liquid chromatography-
608 chemically active liquid core waveguide spectrometry, Anal. Chem., 82, 5838–5843, doi:10.1021/ac101015y, 2010.

609 Gao, Y., Lyu, Y. and Li, X.: Size distribution of airborne particle-bound PAHs and o-PAHs and their implications for
610 dry deposition, Environ. Sci. Process. Impacts, 21, 1184-1192, doi:10.1039/c9em00174c, 2019.

611 Graber, E.R. and Rudich, Y.: Atmospheric HULIS: how humic-like are they? a comprehensive and critical review.
612 Atmos. Chem. Phys. 6, 729–753, doi:10.5194/acp-6-729-2006, 2006.

613 Hallquist, M., Wenger, J.C., Baltensperger, U., Rudich, Y., Simpson, D., Claeys, M., Dommen, J., Donahue, N.M.,
614 George, C., Goldstein, A.H., Hamilton, J.F., Herrmann, H., Hoffmann, T., Iinuma, Y., Jang, M., Jenkin, M.E., Jimenez,
615 J.L., Kiendler-Scharr, A., Maenhaut, W., McFiggans, G., Mentel, Th.F., Monod, A., Prévôt, A.S.H., Seinfeld, J.H.,
616 Surratt, J.D., Szmigielski, R. and Wildt, J.: The formation, properties and impact of secondary organic aerosol: current
617 and emerging issues, Atmos. Chem. Phys., 9, 5155–5236, doi:10.5194/acp-9-5155-2009, 2009.

618 Harrison, M.A.J., Barra, S., Borghesi, D., Vione, D., Arsene, C. and Olariu, R.I.: Nitrated phenols in the atmosphere:
619 a review, Atmos. Environ., 39, 231–248, doi:10.1016/j.atmosenv.2004.09.044, 2005.

620 Havers, N., Burba, P., Lambert, J. and Klockow, D.: Spectroscopic characterization of humic-like substances in
621 airborne particulate matter, J. Atmos. Chem., 29, 45-54, doi:10.1023/A:1005875225800, 1998.

622 Haynes, J. P., Miller, K. E. and Majestic, B. J.: Investigation into photoinduced auto-oxidation of polycyclic aromatic
623 hydrocarbons resulting in brown carbon production, Environ. Sci. Technol., 53, 682-691, doi:10.1021/acs.est.8b05704,
624 2019.

625 Hoffmann, D., Iinuma, Y. and Herrmann, H.: Development of a method for fast analysis of phenolic molecular markers
626 in biomass burning particles using high performance liquid chromatography/atmospheric pressure chemical ionisation
627 mass spectrometry. J. Chromatogr. A, 1143, 168–175, doi:10.1016/j.chroma.2007.01.035, 2007.

https://doi.org/10.5194/acp-2019-673
Preprint. Discussion started: 7 August 2019

Atmospheric Chemistry and Physics Discussions

Huang, W., Huang, B., Bi, X., Lin, Q., Liu, M., Ren, Z., Zhang, G., Wang, X., Sheng, G. and Fu, J.: Emission of PAHs, NPAHs and OPAHs from residential honeycomb coal briquette combustion, Energy & Fuels, 28, 636–642, doi:10.1021/ef401901d, 2014.

IARC: Diesel and gasoline engine exhausts and some nitroarenes, IARC Monographs on the Evaluation of Carcinogenic Risks to Humans, Vol. 46, International Agency for Research on Cancer, Lyon, 1989.

IARC: Diesel and Gasoline Engine Exhausts and Some Nitroarenes, IARC Monographs on the Evaluation of Carcinogenic Risks to Humans, Vol. 105, International Agency for Research on Cancer, Lyon, 2013.

Iinuma, Y., Brüggemann, E., Gnauk, T., Müller, K., Andreae, M.O., Helas, G., Parmar, R., and Herrmann, H.: Source characterization of biomass burning particles: the combustion of selected European conifers, African hardwood, savanna grass, and German and Indonesian peat, J. Geophys. Res., 112, D8209, doi:10.1029/2006JD007120, 2007

Iinuma, Y., Böge, O., Gräfe, R. and Herrmann, H.: Methyl-nitrocatechols: atmospheric tracer compounds for biomass burning secondary organic aerosols, Environ. Sci. Technol., 44, 8453–8459, doi:10.1021/es102938a, 2010.

Iinuma, Y., Keywood, M. and Herrmann, H: Characterization of primary and secondary organic aerosols in Melbourne airshed: the influence of biogenic emissions, wood smoke and bushfires, Atmos. Environ., 130, 54–63, doi:10.1016/j.atmosenv.2015.12.014, 2016.

Inomata, S., Fushimi, A., Fujitani, Y., and Yamada, H.: 4-Nitrophenol, 1-nitropyrene, and 9-nitroanthracene emissions in exhaust particles from diesel vehicles with different exhaust gas treatments, Atmos. Environ., 110, 93-102, doi:10.1016/j.atmosenv.2015.03.043, 2015.

Jaenicke, R.: Aerosol physics and chemistry, Landolt-Börnstein Neue Ser., 4b, 391-457, 1988.

Kahnt, A., Behrouzi, S., Vermeylen, R., Shalamzari, M.S., Vercauteren, J., Roekens, E., Claeys, M. and Maenhaut, W.: One-year study of nitro-organic compounds and their relation to wood burning in PM_{10} aerosol from a rural site in Belgium, Atmos. Environ., 81, 561–568, doi:10.1016/j.atmosenv.2013.09.041, 2013.

Karavalakis, G., Deves, G., Fontaras, G., Stournas, S., Samaras, Z. and Bakeas, E.: The impact of soy-based biodiesel on PAH, nitro-PAH and oxy-PAH emissions from a passenger car operated over regulated and nonregulated driving cycles, Fuel, 89, 3876–3883, doi:10.1016/j.fuel.2010.07.002, 2010.

Kelly, J.L., Michelangeli, D.V., Makar, P.A., Hastie, D.R., Mozurkewich, M. and Auld, J.: Aerosol speciation and mass prediction from toluene oxidation under high NO_x conditions, Atmos. Environ., 44, 361–369, doi:10.1016/j.atmosenv.2009.10.035, 2010.

Kitanovski, Z., Grgić, I., Vermeylen, R., Claeys, M. and Maenhaut, W.: Liquid chromatography tandem mass spectrometry method for characterization of monoaromatic nitro-compounds in atmospheric particulate matter, J. Chromatogr. A, 1268, 35–43, doi:10.1016/j.chroma.2012.10.021, 2012b.

Kitanovski, Z., Grgić, I., Yasmeen, F., Claeys, M. and Čusak, A.: Development of a liquid chromatographic method based on ultraviolet-visible and electrospray ionization mass spectrometric detection for the identification of nitrocatechols and related tracers in biomass burning atmospheric organic aerosol, Rapid Commun. Mass Spectrom., 26, 793-804, doi:10.1002/rcm.6170, 2012a.

Kojima, Y., Inazu, K., Hisamatsu, Y., Okochi, H., Baba, T. and Nagoya, T.: Influence of secondary formation on atmospheric occurrences of oxygenated polycyclic aromatic hydrocarbons in airborne particles, Atmos. Environ., 44, 2873–2880, doi:10.1016/j.atmosenv.2010.04.048, 2010.

Kroflič, A., Grilc, M. and Grgić, I.: Unraveling pathways of guaiacol nitration in atmospheric waters: nitrite, a source of reactive nitronium ion in the atmosphere. Environ. Sci. Technol., 49, 9150-9158, doi:10.1021/acs.est.5b01811, 2015.

Lammel, G.: Polycyclic aromatic compounds in the atmosphere – a review identifying research needs, Polycyclic Aromat. Compd., 35, 316-329, doi:10.1080/10406638.2014.931870, 2015.

Lammel, G., Mulder, M.D., Shahpoury, P., Kukučka, P., Lišková, H., Přibylová, P., Prokeš, R. and Wotawa, G.: Nitro-polycyclic aromatic hydrocarbons - gas-particle partitioning, mass size distribution, and formation along transport in marine and continental background air. Atmos. Chem. Phys., 17, 6257-6270, doi:10.5194/acp-17-6257-2017, 2017.

https://doi.org/10.5194/acp-2019-673
Preprint. Discussion started: 7 August 2019

Atmospheric Chemistry and Physics Discussions

674 Ladji, R., Yassaa, N., Balducci, C., Cecinato, A. and Meklati, B. Y.: Distribution of the solvent-extractable organic
675 compounds in fine (PM1) and coarse (PM1-10) particles in urban, industrial and forest atmospheres of Northern
676 Algeria, Sci. Total Environ., 408, 415-424, doi:10.1016/j.scitotenv.2009.09.033, 2009.

677 Lan, S.H., Lan, H.X., Yang, D. and Wu, X.W.: Study of nitro-polycyclic aromatic hydrocarbons in particulate matter
678 in Dongguan. Environ. Sci. Pollut. Res., 21, 7390-7399, doi:10.1007/s11356-014-2644-y, 2014.

679 Laskin, A., Laskin, J. and Nizkorodov, S.A.: Chemistry of atmospheric brown carbon. Chem. Rev., 115, 4335–4382,
680 doi:10.1021/cr5006167, 2015.

681 Li, Q., Wyatt, A. and Kamens, R. M.: Oxidant generation and toxicity enhancement of aged-diesel exhaust, Atmos.
682 Environ., 43, 1037–1042, doi:10.1016/j.atmosenv.2008.11.018, 2009.

683 Li, X., Jiang, L., Hoa, L.P., Lyu, Y., Xu, T., Yang, X., Iinuma, Y., Chen, J. and Herrmann, H.: Size distribution of
684 particle-phase sugar and nitrophenol tracers during severe urban haze episodes in Shanghai, Atmos. Environ., 145,
685 115–127, doi:10.1016/j.atmosenv.2016.09.030, 2016.

686 Lin, P., Huang, X.F., He, L.Y. and Yu, J.Z.: Abundance and size distribution of HULIS in ambient aerosols at a rural
687 site in South China, J. Aerosol Sci., 41, 74-87, doi:10.1016/j.jaerosci.2009.09.001, 2010.

688 Lin, Y., Ma, Y., Qiu, X., Li, R., Fang, Y., Wang, J., Zhu, Y. and Hu, D.: Sources, transformation, and health
689 implications of PAHs and their nitrated, hydroxylated, and oxygenated derivatives in $PM_{2.5}$ in Beijing, J. Geophys.
690 Res., 120, 7219–7228, doi:10.1002/2015JD023628, 2015.

691 McWhinney, R. D., Gao, S. S., Zhou, S. and Abbatt, J. P. D.: Evaluation of the effects of ozone oxidation on redox-
692 cycling activity of two-stroke engine exhaust particles, Environ. Sci. Technol., 45, 2131–2136,
693 doi:10.1021/es102874d, 2011.

694 Mohr, C., Lopez-Hilfiker, F.D., Zotter, P., Prévôt, A.S.H., Xu, L., Ng, N.L., Herndon, S.C., Williams, L.R., Franklin,
695 J.P., Zahniser, M.S., Worsnop, D.R., Knighton, W.B., Aiken, A.C., Gorkowski, K.J., Dubey, M.K., Allan, J.D. and
696 Thornton J.A.: Contribution of nitrated phenols to wood burning brown carbon light absorption in Detling, United
697 Kingdom during winter time, Environ. Sci. Technol., 47, 6316-6324, doi:10.1021/es400683v, 2013.

698 Neusüss, C., Pelzing, M., Plewka, A. and Herrmann, H.: A new analytical approach for size-resolved speciation of
699 organic compounds in atmospheric aerosol particles: methods and first results. J. Geophys. Res., 105, 4513-4527,
700 doi:10.1029/1999JD901038, 2000.

701 Noguchi, K., Toriba, A., Chung, S.W., Kizu, R., and Hayakawa, K.: Identification of estrogenic/anti-estrogenic
702 compounds in diesel exhaust particulate extract, Biomed. Chromatogr., 21, 1135–1142, doi:10.1002/bmc.861, 2007.

703 Orakij, W., Chetiyanukornkul, T., Kasahara, C., Boongla, Y., Chuesaard, T., Furuuchi, M., Hata, M., Tang, N.,
704 Hayakawa, K. and Toriba, A.: Polycyclic aromatic hydrocarbons and their nitro derivatives from indoor biomass-
705 fuelled cooking in two rural areas of Thailand: a case study, Air Qual. Atmos. Heal., 10, 747–761, doi:10.1007/s11869-
706 017-0467-y, 2017.

707 Özel, M.Z., Hamilton, J.F. and Lewis, A.C.: New sensitive and quantitative analysis method for organic nitrogen
708 compounds in urban aerosol samples, Environ. Sci. Technol., 45, 1497-1505, doi:10.1021/es102528g, 2011.

709 Pavlovic, J. and Hopke, P.K.: Chemical nature and molecular weight distribution of the water-soluble fine and ultrafine
710 PM fractions collected in a rural environment, Atmos. Environ., 59, 264–271, doi:10.1016/j.atmosenv.2012.04.053,
711 2012.

712 Pham, C. T., Kameda, T., Toriba, A. and Hayakawa, K.: Polycyclic aromatic hydrocarbons and nitropolycyclic
713 aromatic hydrocarbons in particulates emitted by motorcycles, Environ. Pollut., 183, 175–183,
714 doi:10.1016/j.envpol.2013.01.003, 2013.

715 Ringuet, J., Leoz-Garziandia, E., Budzinski, H., Villenave, E. and Albinet, A.: Particle size distributions of nitrated
716 and oxygenated polycyclic aromatic hydrocarbons (NPAHs and OPAHs) on traffic and suburban sites of a European
717 megacity: Paris (France). Atmos. Chem. Phys., 12, 8877-8887, doi:10.5194/acp-12-8877-2012, 2012.

718 Seki, K., Noya, Y., Mikami, Y., Taneda, S., Suzuki, A.K., Kuge, Y. and Ohkura, K.: Isolation and identification of
719 new vasodilative substances in diesel exhaust particles. Environ. Sci. Pollut. Res., 17, 717-723, doi:10.1007/s11356-
720 009-0207-4, 2010.

https://doi.org/10.5194/acp-2019-673
Preprint. Discussion started: 7 August 2019

Atmospheric Chemistry and Physics Discussions

Shahpoury, P., Kitanovski, Z. and Lammel, G.: Snow scavenging and phase partitioning of nitrated and oxygenated aromatic hydrocarbons in polluted and remote environments in central Europe and the European Arctic, Atmos. Chem. Phys., 18, 13495–13510, doi:10.5194/acp-18-13495-2018, 2018.

Shen, G., Tao, S., Wei, S., Zhang, Y., Wang, R., Wang, B., Li, W., Shen, H., Huang, Y., Chen, Y., Chen, H., Yang, Y., Wang, W., Wang, X., Liu, W. and Simonich, S. L. M.: Emissions of parent, nitro, and oxygenated polycyclic aromatic hydrocarbons from residential wood combustion in rural China, Environ. Sci. Technol., 46, 8123–8130, doi:10.1021/es301146v, 2012.

Shen, G., Xue, M., Wei, S., Chen, Y., Wang, B., Wang, R., Lv, Y., Shen, H., Li, W., Zhang, Y., Huang, Y., Chen, H., Wei, W., Zhao, Q., Li, B., Wu, H. and Tao, S.: Emissions of parent, nitrated, and oxygenated polycyclic aromatic hydrocarbons from indoor corn straw burning in normal and controlled combustion conditions, J. Environ. Sci., 25, 2072–2080, doi:10.1016/S1001-0742(12)60249-6, 2013a.

Shen, G., Tao, S., Wei, S., Chen, Y., Zhang, Y., Shen, H., Huang, Y., Zhu, D., Yuan, C., Wang, H., Wang, Y., Pei, L., Liao, Y., Duan, Y., Wang, B., Wang, R., Lv, Y., Li, W., Wang, X. and Zheng, X.: Field measurement of emission factors of PM, EC, OC, parent, nitro-, and oxy- polycyclic aromatic hydrocarbons for residential briquette, coal cake, and wood in rural Shanxi, China, Environ. Sci. Technol., 47, 2998–3005, doi:10.1021/es304599g, 2013b.

Shen, G.F., Chen, Y.C., Du, W., Lin, N., Wang, X.L., Cheng, H.F., Liu, J.F., Xue, C.Y., Liu, G.Q., Zeng, E.Y., Xing, B.S. and Tao, S.: Exposure and size distribution of nitrated and oxygenated polycyclic aromatic hydrocarbons among the population using different household fuels, Environ. Pollut., 216, 935-942, doi:10.1016/j.envpol.2016.07.002, 2016.

Song, J.Z., Li, M.J., Jiang, B., Wei, S.Y., Fan, X.J., Peng, P.: Molecular characterization of water-soluble Humic like Substances in smoke particles emitted from combustion of biomass materials and coal using ultrahigh-resolution electrospray ionization Fourier transform ion cyclotron resonance mass spectrometry. Environ. Sci. Technol., 52, 2575–2585, doi:10.1021/acs.est.7b06126, 2018.

Souza, K. F., Carvalho, L. R. F., Allen, A. G. and Cardoso, A. A.: Diurnal and nocturnal measurements of PAH, nitro-PAH, and oxy-PAH compounds in atmospheric particulate matter of a sugar cane burning region, Atmos. Environ., 83, 193–201, doi:10.1016/j.atmosenv.2013.11.007, 2014.

Stevanovic, S., Miljevic, B., Surawski, N. C., Fairfull-Smith, K. E., Bottle, S. E., Brown, R. and Ristovski, Z. D.: Influence of oxygenated organic aerosols (OOAs) on the oxidative potential of diesel and biodiesel particulate matter, Environ. Sci. Technol., 47, 7655-7662, doi:10.1021/es4007433, 2013.

Teich, M., Pinxteren, D. and Herrmann, H.: Determination of nitrophenolic compounds from atmospheric particles using hollow-fiber liquid-phase microextraction and capillary electrophoresis/mass spectrometry analysis, Electrophoresis, 35, 1353–1361, doi:10.1002/elps.201300448, 2014.

Teich, M., van Pinxteren, D., Wang, M., Kecorius, S., Wang, Z., Müller, T., Močnik, G. and Herrmann, H.: Contributions of nitrated aromatic compounds to the light absorption of water-soluble and particulate brown carbon in different atmospheric environments in Germany and China, Atmos. Chem. Phys., 17, 1653-1672, doi:10.5194/acp-17-1653-2017, 2017.

Tomaz, S., Shahpoury, P., Jaffrezo, J.-L., Lammel, G., Perraudin, E., Villenave, E. and Albinet, A.: One-year study of polycyclic aromatic compounds at an urban site in Grenoble (France): seasonal variations, gas/particle partitioning and cancer risk estimation, Sci. Total Environ., 565, 1071–1083, doi:10.1016/j.scitotenv.2016.05.137, 2016.

van Pinxteren, D. and Herrmann, H.: Determination of functionalised carboxylic acids in atmospheric particles and cloud water using capillary electrophoresis/mass spectrometry, J. Chromatogr. A, 1171, 112-123, doi:10.1016/j.chroma.2007.09.021, 2007.

van Pinxteren, D., Teich, M., and Herrmann, H.: Hollow fibre liquid-phase microextraction of functionalised carboxylic acids from atmospheric particles combined with capillary electrophoresis/mass spectrometric analysis, J. Chromatogr. A, 1267, 178-188, doi:10.1016/j.chroma.2012.06.097, 2012

Verma, V., Fang, T., Guo, H., King, L., Bates, J. T., Peltier, R. E., Edgerton, E., Russell, A. G., and Weber, R. J.: Reactive oxygen species associated with water-soluble PM2.5 in the southeastern United States: spatiotemporal trends and source apportionment, Atmos. Chem. Phys., 14, 12915-12930, doi:10.5194/acp-14-12915-2014, 2014.

https://doi.org/10.5194/acp-2019-673
Preprint. Discussion started: 7 August 2019

Atmospheric Chemistry and Physics Discussions

769 Verma, V., Wang, Y., el Afifi, R., Fang, T., Rowland, J., Russell, A.G. and Weber, R.J.: Fractionating ambient humic-
770 like substances (HULIS) for their reactive oxygen species activity - assessing the importance of quinones and
771 atmospheric aging. Atmos. Environ., 120, 351-359, doi:10.1016/j.atmosenv.2015.09.010, 2015.

772 Vicente, E. D., Vicente, A. M., Musa Bandowe, B. A. and Alves, C. A.: Particulate phase emission of parent polycyclic
773 aromatic hydrocarbons (PAHs) and their derivatives (alkyl-PAHs, oxygenated-PAHs, azaarenes and nitrated PAHs)
774 from manually and automatically fired combustion appliances, Air Qual. Atmos. Heal., 9, 653–668,
775 doi:10.1007/s11869-015-0364-1, 2016.

776 Vione, D., Maurino, V., and Minero, C.: Photosensitized humic-like substances (HULIS) formation processes of
777 atmospheric significance: a review, Environ. Sci. Pollut. Res. 21, 11614-11622, doi:10.1007/s11356-013-2319-0,
778 2014.

779 Voliotis A., Prokeš R., Lammel G., and Samara C.: New insights on humic-like substances associated with urban
780 aerosols from central and southern Europe: size-resolved chemical characterization and optical properties. Atmos.
781 Environ., 166, 286-299, doi:10.1016/j.atmosenv.2017.07.024, 2017.

782 Walgraeve, C., Demeestere, K., Dewulf, J., Zimmermann, R. and van Langenhove, H.: Oxygenated polycyclic
783 aromatic hydrocarbons in atmospheric particulate matter: Molecular characterization and occurrence, Atmos. Environ.,
784 44, 1831–1846, doi:10.1016/j.atmosenv.2009.12.004, 2010.

785 Wang, L., Wang, X., Gu, R., Wang, H., Yao, L., Wen, L., Zhu, F., Wang, W., Xue, L., Yang, L., Lu, K., Chen, J.,
786 Wang, T., Zhang, Y., and Wang, W.: Observations of fine particulate nitrated phenols in four sites in northern China:
787 concentrations, source apportionment, and secondary formation, Atmos. Chem. Phys., 18, 4349-4359,
788 doi:10.5194/acp-18-4349-2018, 2018.

789 Wang, X., Gu, R., Wang, L., Xu, W., Zhang, Y., Chen, B., Li, W., Xue, L., Chen, J., and Wang, W.: Emissions of fine
790 particulate nitrate phenols from the burning of five common types of biomass, Environ. Pollut., 230, 405-412,
791 doi:10.1016/j.envpol.2017.06.072, 2017.

792 Wang, Y., Hu, M., Wang, Y., Zheng, J., Shang, D., Yang, Y., Liu, Y., Li, X., Tang, R., Zhu, W., Du, Z., Wu, Y., Guo,
793 S., Wu, Z., Lou, S., Hallquist, M., and Yu, J.: The formation of nitro-aromatic compounds under high NOx-
794 anthropogenic VOCs dominated atmosphere in summer in Beijing, China, Atmos. Chem. Phys., 19, 7649-7665,
795 doi:10.5194/acp-19-7649-2019, 2019.

796 Xie, M.J., Chen, X., Hays, M.D., Lewandowski, M., Offenberg, J., Kleindienst, T.E. and Holder, A.L.: Light
797 absorption of secondary organic aerosol: composition and contribution of nitroaromatic compounds. Environ. Sci.
798 Technol., 51, 11607–11616, doi:10.1021/acs.est.7b03263, 2017.

799 Zhang, X., Hecobian, A., Zheng, M., Frank, N.H. and Weber, R.J.: Biomass burning impact on PM $_{2.5}$ over the
800 southeastern US during 2007: integrating chemically speciated FRM filter measurements, MODIS fire counts and PMF
801 analysis, Atmos. Chem. Phys., 10, 6839–6853, doi:10.5194/acp-10-6839-2010, 2010.

802 Zheng, G., He, K., Duan, F., Cheng, Y. and Ma, Y.: Measurement of humic-like substances in aerosols: a review,
803 Environ. Pollut., 181, 301–314, doi:10.1016/j.envpol.2013.05.055, 2013.

804 Zhuo, S., Du, W., Shen, G., Li, B., Liu, J., Cheng, H., Xing, B. and Tao, S.: Estimating relative contributions of primary
805 and secondary sources of ambient nitrated and oxygenated polycyclic aromatic hydrocarbons, Atmos. Environ., 159,
806 126–134, doi:10.1016/j.atmosenv.2017.04.003, 2017.

807 Zielinska, B., Sagebiel, J., Arnott, W.P., Rogers, C.F., Kelly, K.E., Wagner, D.A., Lighty, J.S., Sarofim, A.F., and
808 Palmer, G.: Phase and size distribution of polycyclic aromatic hydrocarbons in diesel and gasoline vehicle emissions,
809 Environ. Sci. Technol., 38, 2557-2567, doi:10.1021/es030518d, 2004.

https://doi.org/10.5194/acp-2019-673
Preprint. Discussion started: 7 August 2019

Atmospheric Chemistry and Physics Discussions

Table 1. Analytes targeted in this study

Analyte	Abbreviation	Q1
3-Nitrosalicylic acid	3-NSA	182
5-Nitrosalicylic acid	5-NSA	182
4-Nitrocatechol	4-NC	154
4-Nitroguaiacol	4-NG	168
4-Methyl-5-nitrocatechol	4-M-5-NC	168
4-Nitrophenol	4-NP	138
2,4-Dinitrophenol	2,4-DNP	183
3-Methyl-4-nitrophenol	3-M-4-NP	152
3-Methyl-5-nitrocatechol	3-M-5-NC	168
3-Methyl-4-nitrocatechol	3-M-4-NC	168
2-Methyl-4-nitrophenol	2-M-4-NP	152
2-Methyl-3,5-dinitrophenol (Dinitro-ortho-cresol)	DNOC	197
1-Nitronaphthalene	1-NNAP	173.1
2-Nitronaphthalene	2-NNAP	173.1
5-Nitroacenaphthene	5-NACE	199.1
2-Nitrofluorene	2-NFLN	211.1
9-Nitroanthracene	9-NANT	223.1
9-Nitrophenanthrene	9-NPHE	223.1
3-Nitrophenanthrene	3-NPHE	223.1
2-Nitrofluoranthene	2-NFLT	247.1
3-Nitrofluoranthene	3-NFLT	247.1
1-Nitropyrene	1-NPYR	247.1
2-Nitropyrene	2-NPYR	247.1
7-Nitrobenz(a)anthracene	7-NBAA	273.1
6-Nitrochrysene	6-NCHR	273.1
1,3-Dinitropyrene	1,3-N_2PYR	292.1
1,6-Dinitropyrene	1,6-N_2PYR	292.1
1,8-Dinitropyrene	1,8-N_2PYR	292.1
6-Nitrobenz(a)pyrene	6-NBAP	297.1
1,4-Naphthoquinone	1,4-O_2NAP	158.1
9-Fluorenone	9-OFLN	180.1
9,10-Anthraquinone	9,10-O_2ANT	208.1
2-Nitro-9-fluorenone	2-N-9-OFLN	225.1
Benz(a)fluorenone	BaOFLN	230.1
Benz(b)fluorenone	BbOFLN	230.1
Benzanthrone	OBAT	230.1
1,2-Benzanthraquinone	1,2-O_2BAA	258.1

Q1 – *m/z* of ions used for quantification in ESI(−)MS for NMAHs and NCI-MS for N/OPAHs

https://doi.org/10.5194/acp-2019-673
Preprint. Discussion started: 7 August 2019

Atmospheric Chemistry and Physics Discussions

Table 2. Sampling details

	Cut-off diameters (µm)	Sampling date	Sample volume (m^3)
Mainz [a] **49.99° N 8.23° E**	10 - 7.2		
	7.2 - 3	17.-20.11.2015	3402
	3 - 1.5	26.-29.11.2015	4124
	1.5 - 0.95	01.-04.12.2015	4088
	0.95 - 0.49	04.-07.12.2015	4197
	<0.49		
Thessaloniki 40.63°N 22.96° E	10 – 3 [b]	27.-29.1.2016	3228
	3 - 0.95 [b]	08.-10.2.2016	3228
	0.95 - 0.49	16.-18.2.2016	3228
	<0.49	22.-24.2.2016	3172
		17.-19.3.2016	3175

[b] pooled from two impactor stages

https://doi.org/10.5194/acp-2019-673
Preprint. Discussion started: 7 August 2019

Atmospheric Chemistry and Physics Discussions

Table 3. Mean absolute concentrations and mass mixing ratios (in brackets) of HULIS[a] in WSOC[a] as well as of NMAHs and water-soluble (WS) N/OPAHs[b] in HULIS in (a) Mainz and (b) Thessaloniki PM.

a.

Particle size µm	WSOC (µgC m^{-3})	HULIS µg m^{-3} (% C/C)	NMAHs ng m^{-3} (%)	WS N/OPAHs pg m^{-3} (%)
< 0.49	1.14	0.80 (39)	3.41 (0.43)	0.7 (0.0001)
0.49-0.95	0.68	0.31 (25)	1.24 (0.40)	0.2 (0.0001)
0.95-3	0.18	0.09 (28)	0.65 (0.73)	0.3 (0.0003)
3-10	0.12	0.09 (42)	0.27 (0.30)	0.2 (0.0002)
Total	2.07	1.29 (33)	5.58 (0.43)	1.4 (0.0001)

b.

Particle size (µm)	WSOC (µgC m^{-3})	HULIS µg m^{-3} (% C/C)	NMAHs ng m^{-3} (%)	WS N/OPAHs pg m^{-3} (%)
< 0.49	2.02	1.29 (34)	24.0 (1.9)	2.7 (0.0002)
0.49-0.95	1.28	0.83 (34)	13.9 (1.7)	0.7 (0.0001)
0.95-3	0.57	0.35 (32)	6.89 (2.0)	0.5 (0.0001)
> 3	0.33	0.11 (18)	1.87 (1.7)	0.7 (0.0006)
Total	4.20	2.58 (32)	46.6 (1.8)	4.5 (0.0002)

[a] Voliotis et al., 2017
[b] 1,4-O_2NAPs and 1-NNAP (criteria: water solubility > 50 mg L^{-1})

https://doi.org/10.5194/acp-2019-673
Preprint. Discussion started: 7 August 2019

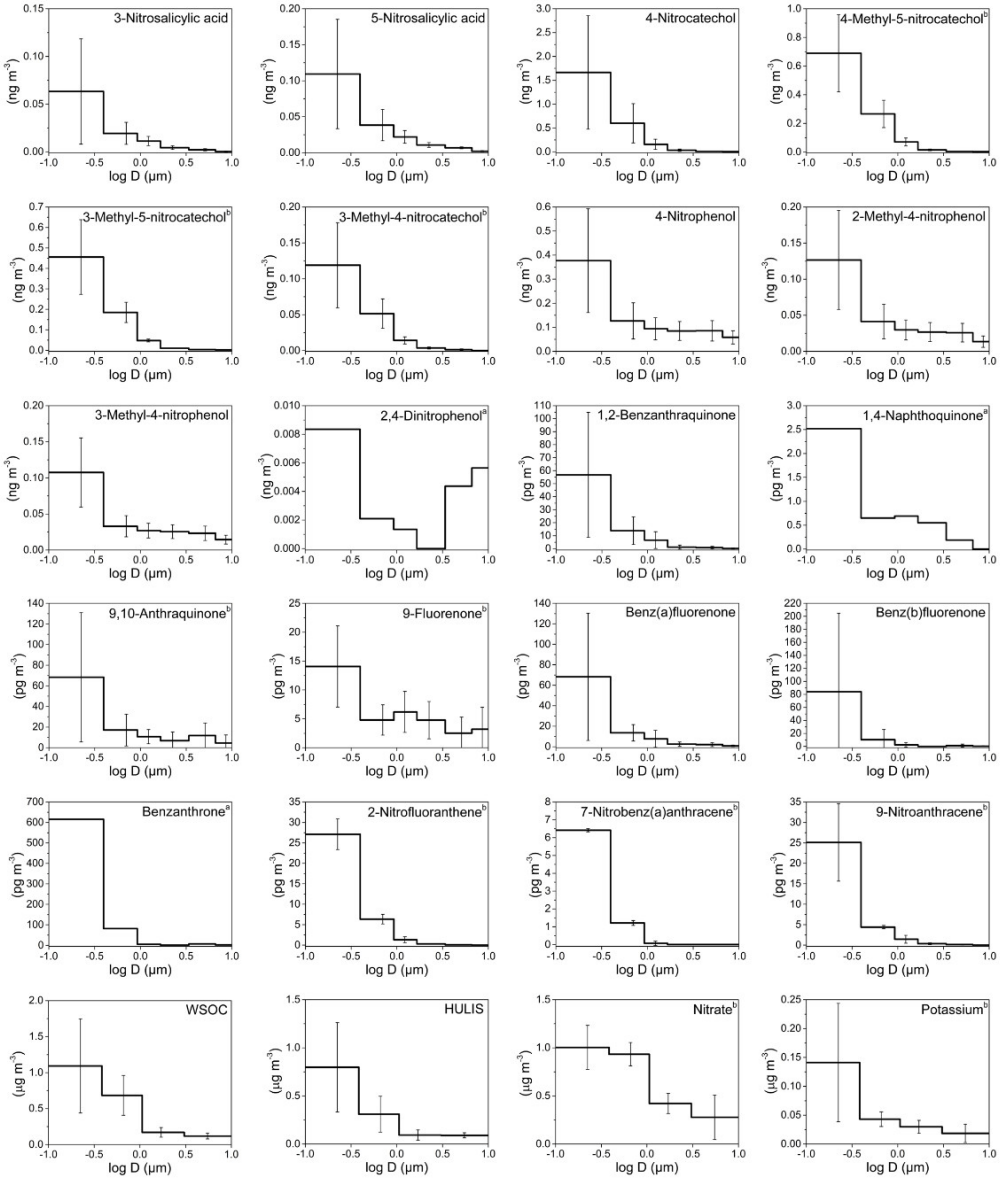

Figure 1. Mass size distributions (MSDs) of PM-bound NMAHs, N/OPAHs, WSOC, HULIS and ions in Mainz (Germany). The error bars represent standard deviations. [a] compound MSD calculated from one (out of four) sample set (detected and quantified in one sample set only); [b] compound MSD calculated from three (out of four) sample sets (detected and quantified in three sample sets only)

https://doi.org/10.5194/acp-2019-673
Preprint. Discussion started: 7 August 2019

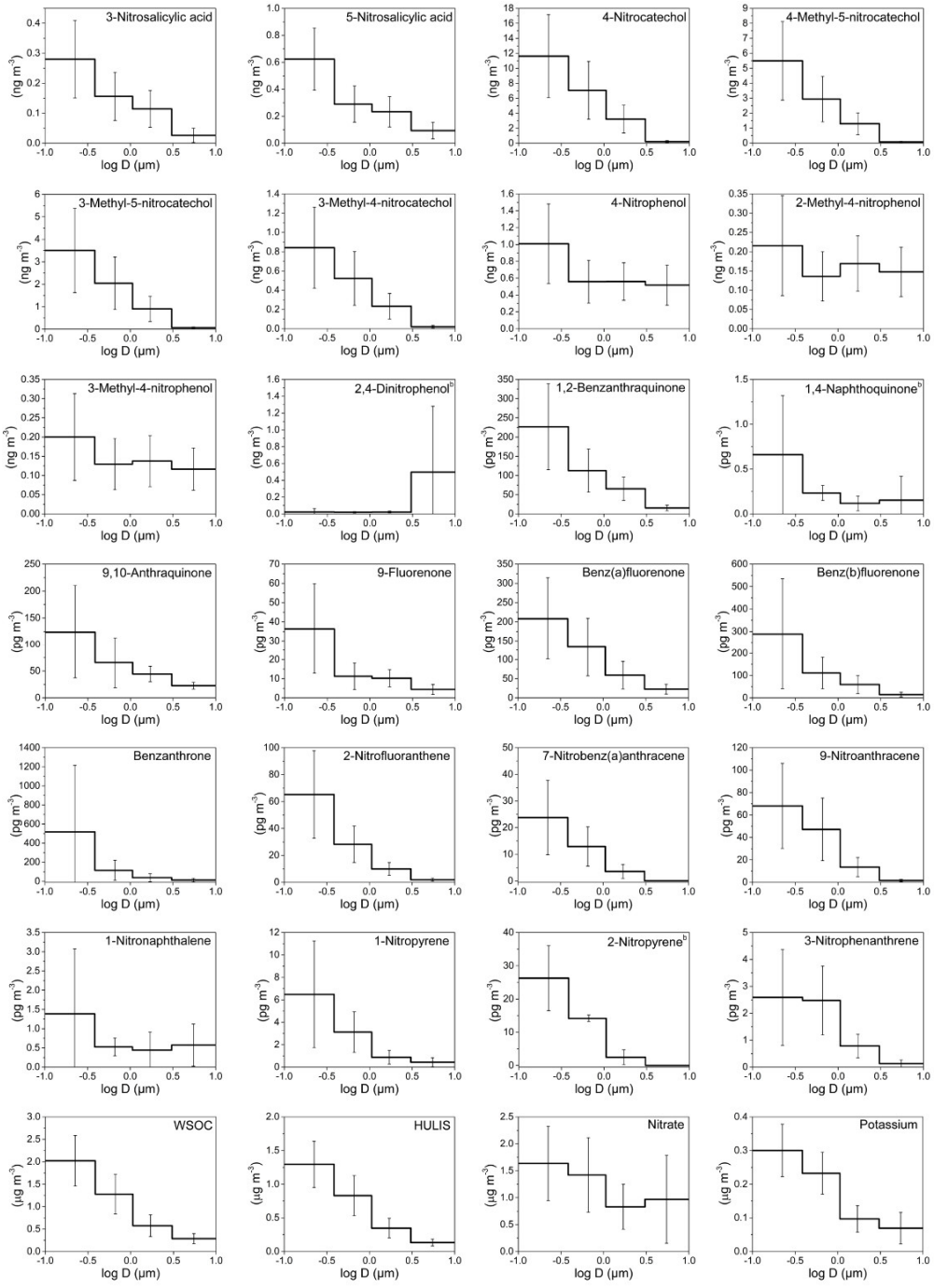

Figure 2. Mass size distributions (MSDs) of PM-bound NMAHs, N/OPAHs, WSOC, HULIS and ions in Thessaloniki (Greece). The error bars represent standard deviations. [b] compound MSD calculated from three (out of five) sample sets (detected and quantified in three sample sets only)